

# tqix: A toolbox for Quantum in X: Quantum measurement, quantum tomography, quantum metrology, and others

Le Bin Ho,<sup>1,2</sup> Kieu Quang Tuan,<sup>3</sup> and Hung Q. Nguyen<sup>4</sup>

<sup>1</sup>*Ho Chi Minh City Institute of Physics, VAST, Ho Chi Minh City, Vietnam*

<sup>2</sup>*Research Institute of Electrical Communication, Tohoku University, Sendai, 980-8577, Japan\**

<sup>3</sup>*University of Science, VNUHCM, Ho Chi Minh City, Vietnam*

<sup>4</sup>*Nano and Energy Center, VNU University of Science,  
Vietnam National University, 120401, Hanoi, Vietnam*

(Dated: February 3, 2021)

We present an open-source computer program written in Python language for quantum measurement and related issues. In our program, quantum states and operators, including quantum gates, can be developed into a quantum-object function represented by a matrix. Build into the program are several measurement schemes, including von Neumann measurement and weak measurement. Various numerical simulation methods are used to mimic the real experiment results. We first provide an overview of the program structure and then discuss the numerical simulation of quantum measurement. We illustrate the program's performance via quantum state tomography and quantum metrology. The program is built in a general language of quantum physics and thus is widely adaptable to various physical platforms, such as quantum optics, ion traps, superconducting circuit devices, and others. It is also ideal to use in classroom guidance with simulation and visualization of various quantum systems.

## I. INTRODUCTION

Quantum measurement theory is a fundamental concept in quantum mechanics in which allows us to predict (i) the probability for obtaining measurement outcomes, and (ii) the post-measurement state conditioned on the obtained outcome [1, 2]. Throughout quantum measurement, the hidden quantum properties will be elucidated to the classical world [3]. It thus plays a crucial role in the characterization of physical systems and immensely vital for the development of quantum technologies, including quantum tomography [4], quantum metrology and quantum imaging [5–7], quantum sensing [8], quantum computing [2, 9, 10], quantum cryptography [11], and others.

On the one hand, quantum measurement and data processing allow for reconstructing the quantum state of the measuring system via a quantum state tomography [4, 12]. Besides, the prediction probability obtained from quantum measurement also reveals the desired parameters that imprint in the measuring system in which one can estimate those parameters via a process called quantum metrology [5, 6]. On the other hand, quantum measurement has wide-range applicability for establishing new quantum technologies such as randomized benchmarking [13], calibrating quantum operations [14], and experimentally validating quantum computing devices [15].

A study on quantum measurement theory is thus increasingly important. Although many physical systems can be carried out experimentally with the current technologies, including quantum optics, ion traps, superconducting circuits, NV center, and NMR devices, ect., it is

still essential for developing an analytical and numerical tool for quantum measurement and data processing. It will be a valuable tool for studying and analyzing various proposed measurement algorithms, enhancing quantum tomography and metrology, and others.

In this work, we construct and develop such a toolbox for quantum measurement and data processing, then apply it to quantum tomography and quantum metrology. We name the program by `tqix`: a toolbox for quantum in X, where X can be the quantum measurement, quantum tomography, quantum metrology, and others. Our program serves as a library for creating and analyzing a quantum system. Indeed, it allows for constructing a quantum object (states and operators), i.e., a library of standard states and operators are build-in `tqix`. Furthermore, various measurement sets [16] have been constructed to manipulate quantum measurement, including Pauli, Stoke, MUB-POVM, and SIC-POVM. Two back-ends for simulating the measurement results are also built. We finally illustrate the code in quantum tomography and quantum metrology using standard data-processing tools, such as trace distance and fidelity.

This program is different from other existing toolboxes, such as Qutip, which focuses on solving the dynamics of open systems [17, 18], and FEYNMAN, which was developed in recent years for the simulation and analysis of quantum registers [19–21] with  $n$ -qubit systems. Here, in this work, we mainly focus on quantum measurement (numerical method and simulation measurement results) and then apply it to enhance quantum tomography and quantum metrology.

The rest of the paper is organized as follows: Section II describes the program's structure. Section III discusses quantum measurement, including some measurement sets and back-ends. Sections IV and V are de-

\* Electronic address: [binho@riec.tohoku.ac.jp](mailto:binho@riec.tohoku.ac.jp)  
Program's website: <https://vqisinfo.wixsite.com/tqix>

voted to quantum tomography and quantum metrology, respectively. In Section VI we discuss the limitation of the program. We conclude our work in section VII, while Appendices are devoted to computational codes used in the main text.

## II. STRUCTURE OF THE PROGRAM

### A. Quantum object

In quantum physics, a system  $\mathcal{S}$  is generally characterized by a preparation quantum state and measuring observables in the Hilbert space. The state is typically represented by a ket vector  $|\psi\rangle$  if it is pure or a density matrix  $\rho$  if it is mixed. Besides, a quantum operator associated with a measurable observable of  $\mathcal{S}$  is described by a Hermitian matrix. They all live in the same Hilbert space  $\mathcal{H}_{\mathcal{S}}$  and obey standard linear algebra.

In `tqix` to represent such a quantum system  $\mathcal{S}$ , we construct a quantum object called `qx`, a matrix representation for quantum state and operators. An illustration of `qx` is given in Fig. 1. A quantum object contains the data about the given state or operator that it represents. Besides providing the data, it also allows us to check its type and dimension using `typex(x)` and `shapex(x)`, respectively. For example, in the following code, we generate a random state in the two-dimensional space and then check its type and dimension.

```
from tqix import *
a = random(2)
print(typex(a))
print(shapex(a))
```

where we get the output as

```
ket
(2, 1)
```

which means it is a ket (column) vector represented by a  $2 \times 1$  matrix.

It is easy to convert a given instance `x`: (integer, real, complex, tuple, array,...) into a quantum object using `qx(x)` command, and its properties can be checked, including bar, ket, oper,... as listed in Table. I. Furthermore, a library of commonly occurring operators is also built into `tqix` as listed in Table. II and allows for operating on the quantum objects. The structure of `qx` is quite similar to the `Qobj` class in Qutip [17, 18].

In subsections IIB and IIC following, we describe detailed quantum states and quantum operators in `tqix`.

### B. Quantum states

It is straightforward to construct quantum states with some standard bases and conventional states that are built into `tqix`. The list of quantum states can be seen

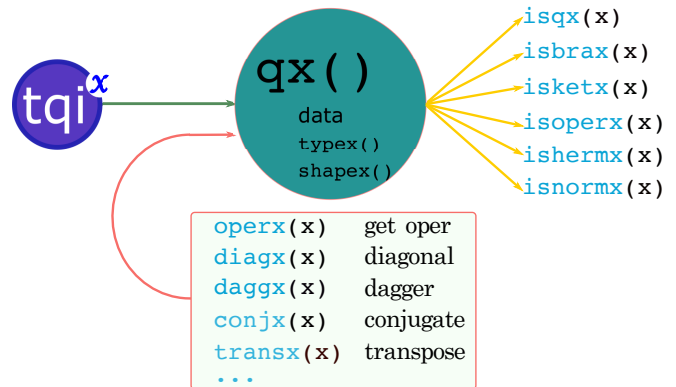


Figure 1. (Color online) Structure of a quantum object in `tqix`. A quantum object can be either a bra-ket vector or a matrix, which stands for quantum states or operators. In `tqix`, a quantum object is represented by a matrix. We can check its physical properties such as type, dimension, Hermiticity, and more (see the full list in Table I). Besides, one can also operate algebra transformations on the quantum object such as conjugate, transpose, and more (see the full list in Table II).

Table I. List of properties of a quantum object. We can easily check the physical properties of a quantum object by using the list below.

Method	Description
<code>isqx(x)</code>	check whether <code>x</code> is a quantum object
<code>isbrax(x)</code>	check whether <code>x</code> is a bra vector
<code>isketx(x)</code>	check whether <code>x</code> is a ket vector
<code>isoperx(x)</code>	check whether <code>x</code> is an operator (mixed state, Hamiltonian,...)
<code>ishermx(x)</code>	check whether <code>x</code> is a Hermit
<code>isnormx(x)</code>	check whether <code>x</code> is normalized

in A. Furthermore, to mimic a real quantum state that may contain systematic errors or technique error, `tqix` allows us to add a small error to the original quantum state:

$$|\psi\rangle \rightarrow |\psi'\rangle = \frac{1}{\mathcal{N}} \sum_n (\psi_n + \delta_n) |n\rangle, \quad (1)$$

where  $\mathcal{N}$  a normalization constant,  $\psi_n = \langle n|\psi\rangle$ , and  $\delta_n$  is a complex random noise following a normal distribution, e.g.,  $\delta_n = a + ib$ , where  $a, b$  are random numbers (noise). For example, we add small random noise into a GHZ state as follows:

```
from tqix import *
import numpy as np

psi = ghz(3)
psip = add_random_noise(psi, m = 0.0, st = 0.1)
```

Here, the random noise obeys a normal distribution with mean `m` and standard deviation `st`, defaulted be zeros. When the noise is presented, the quantum state will de-

Table II. List for commonly occurring operators that are built into `tqix`. We can easily perform these familiar operators on a quantum object.

Method	Description
<code>operx(x)</code>	convert a bra or ket vector into oper
<code>diagx(x)</code>	diagonalize matrix $x$
<code>daggx(x)</code>	get conjugate transpose of $x$ : $x^\dagger$
<code>conjx(x)</code>	get conjugation of $x$ : $x^*$
<code>transx(x)</code>	get transpose of $x$ : $x^T$
<code>tracex(x)</code>	get trace of $x$ : (only for oper)
<code>eigenx(x)</code>	eigenvalue and eigenstate
<code>groundx(x)</code>	get ground state for a given Hamiltonian
<code>expx(x)</code>	exponentiated $x$
<code>sqrtox(x)</code>	square root of $x$
<code>l2normx(x)</code>	get norm 2 of $x$
<code>normx(x)</code>	get normalize of $x$

viate from its original value. Such noisy systems are widespread in various practical situations [22, 23].

For a mixed state, the error can be seen as a white-noise and is given by

$$\rho \rightarrow \rho' = (1 - p)\rho + p\mathbf{I}/d, \quad (2)$$

where  $p$  is a small error ( $0 \leq p \leq 1$ ), and  $d$  is the dimension of the system space. For example, one can easily add a small white noise to an original state (e.g., GHZ state) just with few lines as follows:

```
from tqix import *
rho = ghz(3)
rhop = add_white_noise(rho, p = 0.1)
```

where we have used `p = 0.1` (its default value is zero). The function `add_white_noise` executes Eq. (2) where its input state `rho` can be either pure or mixed state. An identity matrix  $\mathbf{I}$  can be called from `tqix` by `eyex(d)`.

We emphasize that other kinds of error can be defined and constructed by the users themselves, such as bit flip, phase flip, bit-phase flip, depolarizing, amplitude damping, and others (see detailed in Chap. 8 Ref. [2]).

**Visualization of quantum states.** Phase-space representation is a powerful tool to visualize quantum states. Among various ways, the visualization using the Husimi function and Wigner function are two common methods that are widely used [24–27].

In general, a 3-dimension (3D) Husimi function representation of a given state  $\rho$  is  $Q(\alpha) = \frac{1}{\pi} \langle \alpha | \rho | \alpha \rangle$ , where  $|\alpha\rangle$  is the coherent state, and  $\alpha = x + iy$  is a complex number. Similarly, the Wigner function is given by  $W(\alpha) = \frac{2}{\pi} \sum_{k=0}^{\infty} (-1)^k \langle \alpha, k | \rho | \alpha, k \rangle$ , where  $|\alpha, k\rangle = \mathbf{D}(\alpha)|k\rangle$  is the displaced number state, and  $\mathbf{D}(\alpha)$  is the displacement operator [28],

In particular cases of spin systems, it is more convenient to visualize the Husimi and Wigner functions in Bloch spheres. The Husimi function in a Bloch sphere is given by  $Q(\theta, \phi) = \frac{1}{\pi} \langle \theta, \phi | \rho | \theta, \phi \rangle$ , where  $|\theta, \phi\rangle$  is the spin coherent state, and  $\theta, \phi$  are azimuthal and polar angles,

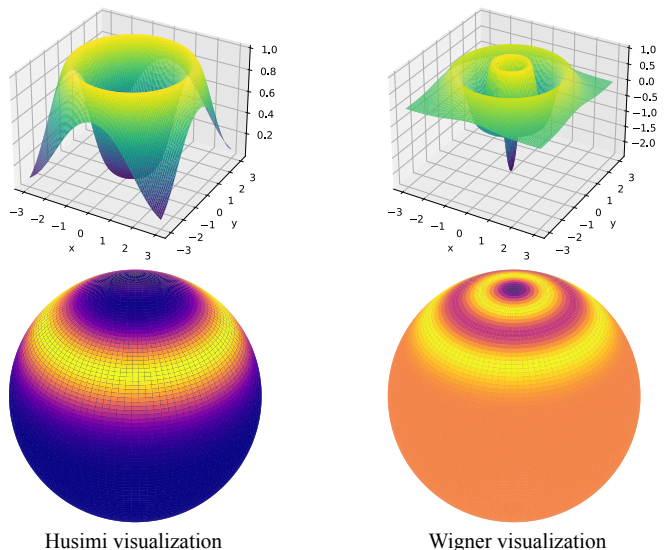


Figure 2. (Color online) The Husimi and Wigner visualizations of a Dicke basis  $|j, m\rangle = |10, 7\rangle$  in 3-dimension (upper row) and in the Bloch sphere (lower row).

respectively. The Wigner function in a Bloch sphere is expressed as [29]

$$W(\theta, \phi) = \sum_{k=0}^{2j} \sum_{q=-k}^k \rho_{kq} Y_{kq}(\theta, \phi) \quad (3)$$

where  $Y_{kq}(\theta, \phi)$  is the spherical harmonic, and  $\rho_{kq} = \sum_{m=-j}^j \sum_{m'=-j}^j \rho_{mm'} t_{kq}^{imm'}$  is the quantum state represented in the spherical harmonics basis [24]. Here,  $\rho_{mm'} = \langle j, m | \rho | j, m' \rangle$  is the quantum state represented in the Dicke basis  $|j, m\rangle$ , and  $t_{kq}^{imm'} = (-1)^{j-m-q} \langle j, m; j, -m' | k, q \rangle$  is the Clebsch-Gordan coefficient [29].

These visualizations are manipulated in `tqix` and are easy to use. For example, in Fig. 2, we visualize the Husimi and Wigner functions of a Dicke basis  $|j, m\rangle$  in 3D and Bloch sphere. The visualization code is shown in III.

### C. Quantum operators

$\mathbf{B}$  represents some standard built-in quantum operators. In `tqix`, a defined operator can be either a Hamiltonian or an evolution operator, represented by a matrix. Also, to manipulate operators' actions on quantum states or operate on multiple states, `tqix` builds various utility mathematical functions, including `dotx` and `tensorx` for dot product and tensor product, respectively.

## D. Construction of quantum systems in `tqix`

With those standard tools presented in subsections II B and II C, we can straightforwardly construct a physical system with the given quantum state and Hamiltonian. For example, one can construct a two-level system state, e.g.,  $1/\sqrt{2}(|0\rangle + |1\rangle)$ , and its unitary evolution, e.g.,  $U = 0.5\sigma_z - 0.25\sigma_x$ , by using the following code:

```
from tqix import *
from numpy import sqrt
state = 1/sqrt(2)*(obasis(2,0) + obasis(2,1))
U = 0.5*sigmaz() - 0.25*sigmax()
evolved_state = dotx(U, state) #U|psi>
```

Composite systems are also easy to create by using the `tensorx` function to generate tensor product states and combine Hilbert spaces. For example, let us consider a three-spin system with the initial state is  $|\uparrow\uparrow\uparrow\rangle$ , and the evolution is  $U = e^{-i\theta\sigma_z\sigma_x\sigma_x}$  where  $\theta$  is a time-dependent phase. One can use the following `tqix` code to generate these objects:

```
from tqix import *
from numpy import pi
theta = pi/4 #for example
up = obasis(2,0) #spin up
state = tensorx(up, up, up)
H = tensorx(sigmaz(), sigmax(), sigmax())
U = exp(-1j*theta*H)
new_state = dotx(U, state)
```

Besides, to decompose a quantum object (state or operator), for example,  $\rho_{AB}$ , on a composite space  $\mathcal{H}_A \otimes \mathcal{H}_B$ , onto a quantum object  $\rho_A$  on  $\mathcal{H}_A$ , we can perform a partial trace using `ptracex` syntax. It is a linear map  $\rho_A = \text{tr}_B[\rho_{AB}]$ :  $AB \rightarrow \text{tr}(B)A$ , for any matrices  $A, B$  on  $\mathcal{H}_A$  and  $\mathcal{H}_B$ , respectively. For example, one can trace out the second and third subsystems of the above Hamiltonian by using

```
H1 = ptracex(H, [2, 3])
```

Here, we keep the first subsystem. Notable that in this version, `ptracex` is only applicable for qubits systems.

## III. QUANTUM MEASUREMENT

`tqix` mainly focuses on the calculation and simulation of quantum measurement for quantum systems. We first review the quantum measurement theory using the POVM formalism and then describe how this measurement is built into `tqix`. For simulating the measurement results, we also construct two available back-ends that can be executed in `tqix`.

### A. General measurement

Quantum measurement is characterized by a set of measurement operators denoted by  $\{M_k\}$  satisfying the

completeness condition  $\sum_k M_k^\dagger M_k = \mathbf{I}$ , where  $k$  is a measurement outcome. These measurement operators will operate on the quantum state of the measuring system. For a quantum system given in a general density state  $\rho$ , the probability to obtain the outcome  $k$  is

$$p_k = \text{tr}[M_k^\dagger M_k \rho]. \quad (4)$$

The quantum state after measurement will collapse to

$$\rho' = \frac{M_k \rho M_k^\dagger}{\text{tr}[M_k^\dagger M_k \rho]}. \quad (5)$$

Furthermore, a projective measurement  $\Pi$  is a special class of the general measurement that described by a Hermitian operator decomposing to

$$\Pi = \sum_k k \Pi_k, \quad (6)$$

where  $\Pi_k \equiv |k\rangle\langle k|$  is a projection operator projected onto the eigenstate  $|k\rangle$  of  $\Pi$  with eigenvalue  $k$ . For a projective measurement, the probability and the post-measurement state are calculated to be:

$$p_k = \text{tr}[\Pi_k \rho], \text{ and } \rho' = \frac{\Pi_k \rho \Pi_k}{\text{tr}[\Pi_k \rho]}. \quad (7)$$

See Ref. [2] for more detailed quantum measurement.

### B. Positive-Operator-Valued Measurement

In many practical cases, such as quantum tomography and quantum metrology, one may not need to care about the post-measurement state but rather focus on the measurement probability. In such cases, analyzing the measurement using a positive-operator-valued measure (POVM) is referred. POVM is a mathematical description of the measurement which is a consequence of the general measurement [2]. A POVM's element, said  $E_k$ , is associated with the measurement  $M_k$  by  $M_k = W\sqrt{E_k}$ , where  $W$  an arbitrary unitary operator, or we can define

$$E_k = M_k^\dagger M_k, \quad (8)$$

that is a positive operator satisfying the completeness relation  $\sum_k E_k = \mathbf{I}$ . The probability, in this case, is given by

$$p_k = \text{tr}[E_k \rho]. \quad (9)$$

The POVM formalism is thus convenient for studying the statistics of the measurement without acknowledging the post-measurement state.

**Pauli measurement set.** In quantum measurements, one can usually combine several POVMs as a measurement set for characterizing properties of the system to

be measured. One common choice is the Pauli measurement set. For one qubit, a measurement set  $M$  consists of three POVMs as

$$\{M\} = \left\{ |H\rangle\langle H|, |V\rangle\langle V|, |D\rangle\langle D|, |A\rangle\langle A|, |L\rangle\langle L|, |R\rangle\langle R| \right\}, \quad (10)$$

where

$$|H\rangle = \begin{pmatrix} 1 \\ 0 \end{pmatrix}, \quad |V\rangle = \begin{pmatrix} 0 \\ 1 \end{pmatrix},$$

$$|D\rangle = \frac{1}{\sqrt{2}} \begin{pmatrix} 1 \\ 1 \end{pmatrix}, \quad |A\rangle = \frac{1}{\sqrt{2}} \begin{pmatrix} 1 \\ -1 \end{pmatrix},$$

and,

$$|L\rangle = \frac{1}{\sqrt{2}} \begin{pmatrix} 1 \\ i \end{pmatrix}, \quad |R\rangle = \frac{1}{\sqrt{2}} \begin{pmatrix} 1 \\ -i \end{pmatrix},$$

therein,  $\{|H\rangle\langle H|, |V\rangle\langle V|\}$ ;  $\{|D\rangle\langle D|, |A\rangle\langle A|\}$ ; and  $\{|L\rangle\langle L|, |R\rangle\langle R|\}$  are the three POVMs. For an  $n$ -qubit system, the measurement set is formed by a tensor product of elements in  $M$ . There are  $6^n$  elements in total, and thus it consumes much calculation cost and the experimental time.

**Stoke measurement set.** Another practical measurement set is based on a light beam's polarization state, which was pioneering proposed by Stoke [30]. He showed that a single qubit system could be determined by a set of four projection measurements. These projection measurements can be chosen arbitrarily from six elements above [12, 31]. In `tgix`, we choose  $|H\rangle\langle H|, |V\rangle\langle V|, |D\rangle\langle D|$ , and  $|R\rangle\langle R|$ .

Likewise the Pauli measurement set, all the elements of  $n$ -qubit system can be found by using a tensor product of four projection measurements, which results in  $4^n$  elements.

**MUB-POVM set.** Given two orthonormal bases  $\{|e_i\rangle\}$  and  $\{|f_j\rangle\}$  in a finite-dimensional Hilbert space  $\mathcal{H}_d$ , they are said to be mutually unbiased (MUB) if the inner product between any two elements in each basis is a constant [32]:

$$|\langle e_i | f_j \rangle|^2 = \frac{1}{d}, \forall i, j \in [1, d]. \quad (11)$$

For a  $d$ -dimensional Hilbert space, in general, there are  $d + 1$  POVMs and  $d$  elements in each POVM. In total, it needs at least  $d^2 - 1$  measurements, which is much smaller than the Pauli case.

There are several methods for finding MUB-POVMs across dimension  $d$ , including the Weyl group [33], unitary operators [34], and the Hadamard matrix method [33]. However, we omit writing them out here and encourage readers to refer [33–37] if needed. In `tgix`, we have constructed several MUB-POVMs for  $d =$

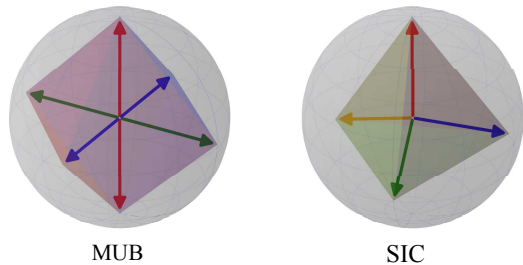


Figure 3. (Color online) Bloch sphere representation of the MUB (a) and SIC (b) measurement sets for one qubit. Six measurements of MUB correspond to vertices of an octahedron, while four measurements of SIC correspond to vertices of a tetrahedron.

2, 3, 4, 5, 7. In the future, we also plan to develop other cases.

**SIC-POVM set.** In a similar manner, a measurement set  $\{|h_i\rangle\}$  is called symmetric informationally complete (SIC) when all the inner products between different elements are equal, and their projectors are complete [38]:

$$|\langle h_i | h_j \rangle|^2 = \frac{1}{d+1}, \forall i \neq j. \quad (12)$$

Notable that there is only one POVM in a SIC-POVM set with  $d^2$  elements.

A most general way to construct a SIC-POVM is using the Weyl-Heisenberg displacement operators [39–41]:

$$D_{j,k} = \omega_d^{jk/2} \sum_{m=0}^{d-1} \omega_d^{jk} |k+m \pmod{d}\rangle \langle m|, \quad (13)$$

where  $\omega_d = \exp(2\pi i/d)$ . Then, a set of SIC-POVM elements can be calculated by applying the displacement operators on the fiducial vector  $|\phi_d\rangle$ . The fiducial vector construction has been carried out so far [38, 40, 42–45] and is listed in [46]. Such a list is also built into `tgix`.

Besides the Pauli and Stoke measurement sets, the MUB-POVM and SIC-POVM measurement sets are also widely used in quantum theory [41, 43, 47–51]. In Fig. 3, we present a Bloch sphere representation of the two MUB and SIC measurement sets for one qubit ( $d = 2$ ). Note that for one qubit, the Pauli measurement set is the same as the MUB one. Six elements of MUB correspond to vertices of an octahedron, while four elements of SIC correspond to vertices of a tetrahedron.

### C. Quantum measurement in `tgix`

In `tgix`, one can calculate the probability for a given quantum system state and a set of observables (or POVMs) as the following example:

```
from tgix import *
state = ghz(1)
```

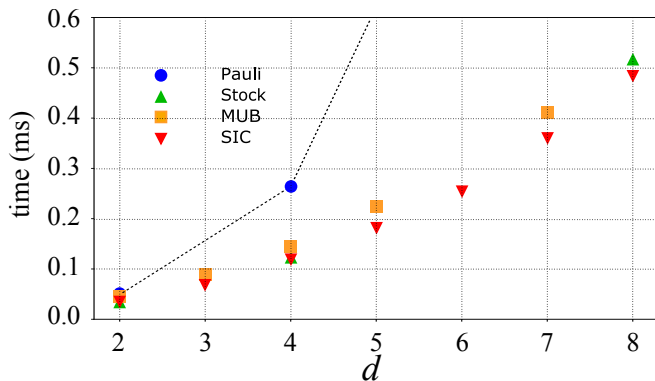


Figure 4. (Color online) The calculation time of different measurement sets. While Pauli measurement consumes much time, Stoke and MUB-POVM have an equivalence time, and SIC-POVM less consumes the time.

```
model = qmeas(state, [sigmax(), sigmay(),
                    sigmaz()])
print(model.probability())
```

In this example, we calculate the expectation values  $\langle \sigma_x \rangle$ ,  $\langle \sigma_y \rangle$ , and  $\langle \sigma_z \rangle$  of a given state  $|\psi\rangle = 1/\sqrt{2}(|0\rangle + |1\rangle)$ . The outcomes are

```
[1.0, 0.0, 0.0]
```

Furthermore, `tcqix` also contains the Pauli, Stoke, MUB-POVM, and SIC-POVM measurement sets. One can easily call them out by a simple syntax, such as

```
model = qmeas(state, 'Pauli')
```

For other measurement sets, one can replace `'Pauli'` by `'Stoke'`, `'MUB'`, and `'SIC'`, respectively.

In Fig. 4, we compare the calculation time of different measurement sets for a random state in  $d$  dimension. Particularly, we first generate a random quantum state. We then measure this state via different measurement sets, i.e., Pauli, Stoke, MUB-POVM, and SIC-POVM, and compare the execution time for each number of dimension  $d$ . See IV for detailed code.

#### D. Back-end for simulation measurement results

A back-end is defined either as a simulator or a real device. For a given quantum object and a set of POVMs, a back-end is executed to simulatively retrieve the corresponding measurement results. In `tcqix`, to mimic the real experiment data, we use several back-ends to simulate the results. A so-called Monte Carlo [52] (`mc`) back-end and Cumulative Distribution Function [53] (`cdf`) back-end have been built into `tcqix`. In the future, we will also construct such a back-end from real devices.

**mc back-end.** Particularly, a straightforward simulation back-end used in `tcqix` is based on the Monte

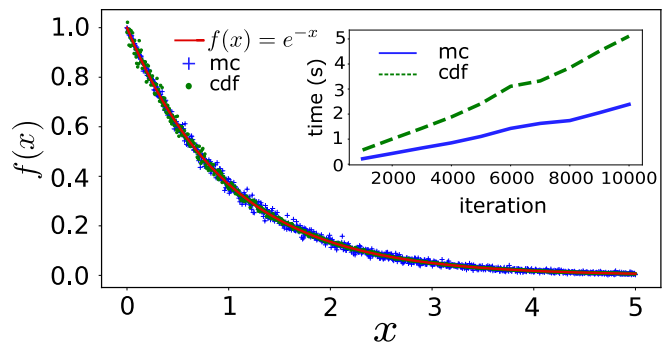


Figure 5. (Color online) Plot of  $f(x)$  versus mc and cdf back-ends. Inset: the simulation time for mc and cdf back-ends. While the cdf back-end is more accurate than the mc back-end, it also consumes more time than the mc one.

Carlo simulation method, which we named as `mc` back-end. Assume that a probability distribution of measurement is  $f(x)$ , generally, a function of  $x$ . Without loss of generality, we assume that  $0 \leq f(x) \leq 1, \forall x$ , (a physical probability does not exceed the range of  $[0, 1]$ .) For each given  $f(k), k \in \{x\}$ , the following procedure is processed: (i) generate a random number  $r$  following a uniform distribution within  $[0, 1]$ , (ii) accept  $r$  if  $r \leq f(k)$ , (iii) repeat (i, ii)  $N_c$  times to get the frequency between the number of accepted  $r$  and  $N_c$ , which will distribute according to  $f(k)$ . This method has been used in quantum state tomography, for example, see Refs. [54, 55].

**cdf back-end.** Another back-end is named as `cdf` based on the cumulative distribution function (cdf). For a given probability distribution of a measurement  $f(x)$ , the cdf function is defined to be

$$F(y) = \int_{-\infty}^y f(x) dx. \quad (14)$$

Given a uniform random variable  $r \in [0, 1]$  then  $y = F^{-1}(r)$  is distributed following  $f(x)$ . Like the `mc` back-end, this method has also been widely used in quantum state tomography [56–59].

As an example, let us choose  $f(x) = e^{-x}, x > 0$ , and therefore the cumulative distribution is  $F(y) = 1 - e^{-y}$ . Then, for a random number  $r$ , the corresponding  $y$  yields:

$$y = -\ln(1 - r), \quad (15)$$

which distributes according to  $f(x)$ .

In Fig. 5, we plot  $f(x)$  and its simulation results via the `mc` and `cdf` back-ends. Refer to V for detailed coding. While the `cdf` back-end is more accurate than the `mc`, the cost that one has to pay is that it consumes more time than the `mc` back-end (see the inset figure.) For some simulation tasks that require sufficient accuracy, we encourage the users to employ the `cdf` back-end.

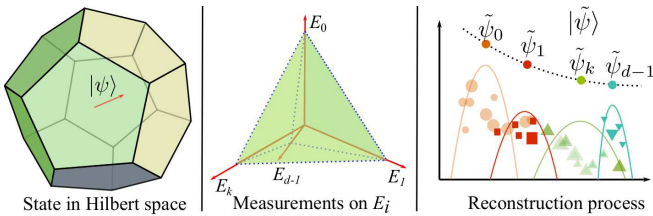


Figure 6. (Color online) Quantum state tomography process: (i) A quantum state  $|\psi\rangle$  is unknown and expressed in its Hilbert space of  $d$  dimension. (ii) The state is measured in a measurement set given by  $E_0, E_1, \dots$ . (iii) The measurement results provide the information of the measuring state via an estimator, such as ML, LS, and so forth. The reconstructed state is  $|\tilde{\psi}\rangle = \sum \tilde{\psi}_n |n\rangle$ .

#### IV. QUANTUM STATE TOMOGRAPHY

In general, the quantum state tomography (QST) is a process that reconstructing the information of unknown quantum states from the measurement data [4]. The tomography procedure is illustrated in Fig. 6. A quantum state, for example  $|\psi\rangle$ , is presented in its Hilbert space as given on the left side of the figure. Here, for a  $d$ -dimensional Hilbert space, the state is expressed by

$$|\psi\rangle = \sum_{n=0}^{d-1} \psi_n |n\rangle, \quad (16)$$

where  $\psi_n$  are unknown parameters need to be estimated, and  $\{|n\rangle\}$  is a computational basis on the Hilbert space. The state is measured in a measurement set, e.g.,  $\{E_0, E_1, \dots\}$  as illustrated in the middle of Fig. 6. The measurement set can be chosen from one of those described in Sec. III. Finally, the measurement results will be analyzed via an estimator such as maximum likelihood (ML) [60], least squares (LS) [12], neural network [61–66], and others, to reproduce the state. The reconstructed state is denoted by  $|\tilde{\psi}\rangle$ , where

$$|\tilde{\psi}\rangle = \sum_{n=0}^{d-1} \tilde{\psi}_n |n\rangle. \quad (17)$$

To evaluate the accuracy of the tomography process, one can compare the true state  $|\psi\rangle$  and the reconstructed state  $|\tilde{\psi}\rangle$  via the various figure of merits such as the trace distance and the fidelity. The trace distance between  $|\psi\rangle$  and  $|\tilde{\psi}\rangle$  is given by

$$D(\psi, \tilde{\psi}) = \sqrt{1 - |\langle \tilde{\psi} | \psi \rangle|^2}. \quad (18)$$

For general mixed states  $\rho$  and  $\tilde{\rho}$ , the trace distance is given by [2]

$$D(\rho, \tilde{\rho}) = \frac{1}{2} \text{tr} |\tilde{\rho} - \rho|. \quad (19)$$

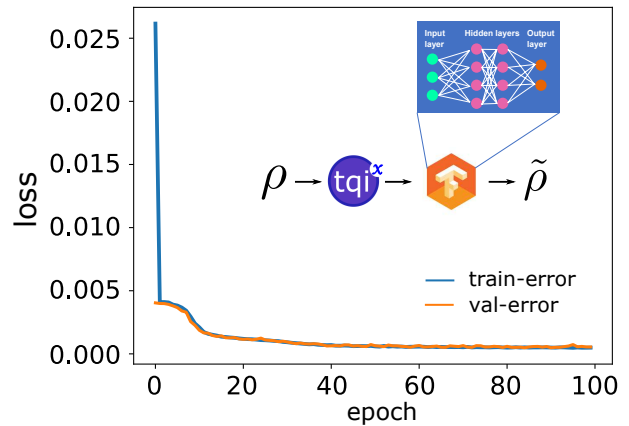


Figure 7. (Color online) Test of loss function for training data and validation data in Tensorflow. There is no overfitting in this example (the training error and the validation error are close.) Inset: tomography scheme: given an unknown state  $\rho$ , through `tfqix`, we obtain the set of measurement results that can be fed into a neural network build-in Tensorflow. From the Tensorflow's output, we can reconstruct the given quantum state, named as  $\tilde{\rho}$ .

Moreover, the fidelity is given by [2]

$$F(\rho, \tilde{\rho}) = \text{tr} \sqrt{\sqrt{\rho} \tilde{\rho} \sqrt{\rho}}. \quad (20)$$

Now, we give an example of using `tfqix` in QST. Assume that a given system is described by a quantum state  $\rho$  that we want to reconstruct. Using `tfqix` as given in Sec. III C, we can get the measurement probabilities. From those measurement data, we reproduce the quantum state. Here, in this example, we use a neural network scheme to reconstruct the quantum state, which is also widely used recently in the QST [61–66]. We build a neural network consists of four layers: an input layer, two hidden layers, and an output layer using Tensorflow. The input layer was fed by the set of outcome probabilities obtained from `tfqix`, while the output layer is the quantum state of being reconstructed. These layers were connected via a `tanh` cost function. Our scheme is illustrated in the inset Fig. 7. In Fig. 7, we also show an example of the loss model while training the experiment data from `tfqix` with the Pauli measurement set.

Besides, `tfqix` also has been used to reconstruct the quantum state using the direct state measurement (DSM) method. For references, we encourage readers to see Refs. [57–59].

#### V. QUANTUM METROLOGY

Quantum metrology is a process that unknown (single or multiples) parameters are estimated from a set of measurements [5, 6]. The process is illustrated in Fig. 8 for a

single parameter estimation. First, a system is prepared in a general mixed density state  $\rho$ . The state will acquire a phase  $\varphi$  after being exposed under an external field represented by a unitary transformation  $\mathbf{U}(\varphi) = e^{-i\varphi\mathbf{H}}$  and transforms to  $\rho(\varphi) = \mathbf{U}(\varphi)\rho\mathbf{U}^\dagger(\varphi)$ . Here,  $\mathbf{H}$  is a generic Hermitian operator. The system after that will be measured via a POVM  $\{E_k\}$ , and the results allow for estimating the unknown parameter  $\varphi$ .

The measurement precision (variance)  $\Delta\varphi$  after  $N$  independent measurements is defined by  $\Delta\varphi = \sqrt{\langle(\varphi - \tilde{\varphi})^2\rangle}$ , where  $\tilde{\varphi}$  is the estimated value. The minimum of  $\Delta\varphi$  is bounded by the Cramér-Rao bounds

$$\Delta\varphi \geq \frac{1}{\sqrt{NF}} \geq \frac{1}{\sqrt{NQ}}, \quad (21)$$

where  $F$  and  $Q$  are the classical and quantum Fisher information, respectively, which are defined by [67]

$$F = \sum_k \frac{1}{p_k(\varphi)} \left[ \frac{\partial p_k(\varphi)}{\partial \varphi} \right]^2, \quad (22)$$

$$Q = 2 \sum_{m,n} \frac{(q_m - q_n)^2}{q_m + q_n} |\langle m | \mathbf{H} | n \rangle|^2. \quad (23)$$

Here, the probability of a measurement  $E_k$  is given by  $p_k(\varphi) = \text{tr}[E_k \rho(\varphi)]$ , as in Eq. (7), and the density state  $\rho(\varphi)$  is given in its spectral decomposed form, i.e.,  $\rho(\varphi) = \sum_m q_m |m\rangle\langle m|$ , where  $q_m$  and  $|m\rangle$  are eigenvalues and eigenvectors, respectively.

The first inequality in Eq. 21 is classical Cramér-Rao bound (CCRB) while the second one is quantum Cramér-Rao bound (QCRB). In the single parameter estimation, the CCRB is saturated by the maximum likelihood estimator asymptotically in the number of repeated measurements [ $N$  in Eq. (21)], and the QCRB is saturated by using an optimal measurement observable, which is given by the projection over the eigenstates of the symmetric logarithmic derivatives (SLD) (see Refs. [5, 6, 67, 68]). Furthermore,  $\Delta\varphi$  reaches the standard quantum limit (SQL) precision scaling if it is proportional to  $1/\sqrt{N}$ , while it reaches the Heisenberg limit (HL) when  $\Delta\varphi \propto 1/N$ .

Hereafter, we provide an example for studying quantum metrology using `qtix`. In our example, we consider a cat state quantum system, which is the superposition of spin- $j$  coherent states [69, 70]

$$|\psi\rangle = \mathcal{N} \left( |\theta, \phi\rangle + |\pi - \theta, \phi\rangle \right), \quad (24)$$

where  $\mathcal{N}$  is the normalization constant and  $|\theta, \phi\rangle$  is a spin- $j$  coherent state [71]

$$|\theta, \phi\rangle = \sum_{m=-j}^j c_m \cos^{j+m} \left( \frac{\theta}{2} \right) \sin^{j-m} \left( \frac{\theta}{2} \right) e^{-i(j-m)\phi} |j, m\rangle, \quad (25)$$

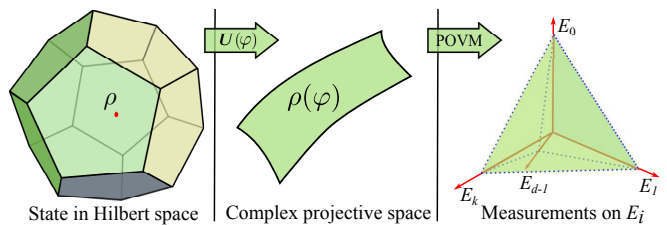


Figure 8. (Color online) Quantum metrology process: (i) A quantum system given in its density state  $\rho$ . (ii) The system is exposed under an external field given by  $\mathbf{U}(\varphi)$  where  $\varphi$  is an unknown field parameter and becomes  $\rho(\varphi)$ . (iii) The state  $\rho(\varphi)$  is measured in a measurement set given by  $E_0, E_1, \dots$  and provides the information on the estimated parameter  $\varphi$ .

where  $c_m = \sqrt{\frac{(2j)!}{(j+m)!(j-m)!}}$ . Without loss of generality, we can choose  $\phi = 0$ . Here,  $|j, m\rangle$  is the standard angular momentum basis with the angular momentum quantum number  $j = 0, 1/2, 1, \dots$ , and  $m = -j, -j+1, \dots, j$  [72].

Under the transformation  $\mathbf{U}(\varphi) = e^{-i\varphi\mathbf{S}_z}$ , the system evolves to  $|\psi(\varphi)\rangle = \mathbf{U}(\varphi)|\psi\rangle$ . We then, evaluate the measurement precision by [73]

$$\Delta\varphi = \frac{\sqrt{\langle\mathbf{S}_y^2\rangle - \langle\mathbf{S}_y\rangle^2}}{|\partial\langle\mathbf{S}_y\rangle/\partial\varphi|}, \quad (26)$$

where  $\mathbf{S}_k$  ( $k = x, y, z, +, -$ ) is a spin operator.

In Fig. 9, we show the expectation values  $\langle\mathbf{S}_y\rangle$  (a) and  $\Delta\varphi$  (b) as functions of  $\varphi$ . Here, we examine several values of  $\theta$  as shown in the figure. We can see that the variance  $\Delta\varphi$  can reach the minimum at an optimized value for  $\varphi$ . We emphasize that  $\varphi$  is a function of the exposing time (the time that we expose the system under the external field), and thus there exists an optimal time that the variance is minimum. Interestingly, we can see that for  $\theta = 0.0$  and  $0.15\pi$  the minimum variance can beat the SQL. This example is in agreement with Ref. [73]. The code for generating Fig. 9 is shown in VI.

## VI. LIMITATION OF THE PROGRAM

Within the initial version of the program, we cannot cover all the existing quantum objects (quantum states and operators) here. We limit ourselves to some basic and useful quantum objects as mentioned throughout the paper. Further developed versions will improve and complement these lacking parts.

In quantum measurement, the program limits on some practical POVM sets, such as Pauli, Stoke, MUB-POVM, and SIC-POVM measurement sets, which are widely used in quantum theory and can be carried out in various experiments. Besides, the MUB-POVM has been constructed for  $d = 2, 3, 4, 5, 7$ , where higher dimensions



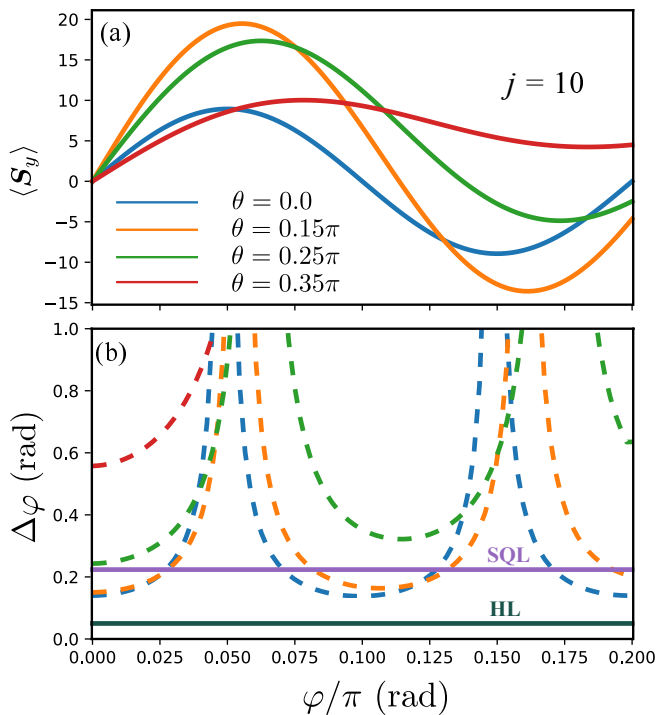


Figure 9. (Color online) (a) Plot of expectation value  $\langle S_y \rangle$  as a function of  $\varphi$ . We show the results for several values of  $\theta$  as in the figure. Here we fix  $j = 10$ . (b) Plot of the variance  $\Delta\varphi$  as a function of  $\varphi$ . Several results are plotted with the same  $\theta$  in (a). The SQL and HL are also shown in the figure.

(to our knowledge) do not exist yet.

In the context of quantum tomography, the example

program is limited to getting meaningful quantum states such as GHZ, W, and Dicke states. However, we emphasize that the program can be used for estimating any given quantum states, including non-classical states, such as coherent state, squeezed state, spin-coherent state, and others. Here, we highlight several example calculations to provide the readers with an overview of the program. Various tutorials can be found on the websites.

## VII. CONCLUSION

We have presented a computer program `tqix` by using the Python programming language and applied to the quantum measurement, quantum tomography, and quantum metrology. In this work, we have constructed a basic structure and some quantum features of a quantum object which can be used for both quantum states and quantum observables. There are several back-ends have been constructed for simulation in quantum measurement. Thus, this program is applicable for a spacious range in quantum measurement, quantum tomography, and quantum metrology. We strongly encourage those who have used this program to feedback (if any) error or incorrect to us for further developing the program.

## ACKNOWLEDGMENTS

This work was supported by JSPS KAKENHI Grant Number 20F20021 and the Vietnam National University under Grant Number QG.20.17.

## Appendix A: List of quantum states build-in `tqix`

In this appendix, we summary some useful quantum states used in the program. In the future, we also build other quantum states to the code.

Table III. List of quantum states are built-in tqix

Name	Description
<code>obasis(d, k)</code>	orthogonal basis with $d$ -dimension, excited at $k$ , such as <code>obasis(3,0)</code> $= \begin{pmatrix} 1 \\ 0 \\ 0 \end{pmatrix}$ , <code>obasis(3,1)</code> $= \begin{pmatrix} 0 \\ 1 \\ 0 \end{pmatrix}$ , ...
<code>dbasis(d, k)</code>	dual basis for the basis <code>obasis</code>
<code>zbasis(j, m)</code>	Zeeman basis or Dicke basis $ j, m\rangle$ with spin number $j$ and quantum number $m \in [-j, j]$ .
<code>dzbasis(j, m)</code>	dual basis for the Zeeman basis <code>zbasis</code> .
<code>coherent(d, alpha)</code>	generating coherent state that cut off at $d$ dimension: $ \alpha\rangle = e^{-\frac{ \alpha ^2}{2}} \sum_{n=0}^d \frac{\alpha^n}{\sqrt{n!}}  n\rangle$ , where $\alpha$ is a complex number provided by <code>alpha</code> , and $\{ n\rangle\}$ is the Fock (number) basis.
<code>squeezed(d, alpha, beta)</code>	generating squeezed coherent state that cut off at $d$ dimension: $ \alpha, \beta\rangle = e^{\alpha\mathbf{a}^\dagger - \alpha^* \mathbf{a}} e^{\frac{1}{2}(\beta^* \mathbf{a}^2 - \beta \mathbf{a}^{\dagger 2})}  0\rangle$ , where $\mathbf{a}, \mathbf{a}^\dagger$ are annihilation and creation operators, respectively; $\alpha, \beta$ are complex numbers.
<code>position(d, x)</code>	generating position state which is an eigenstate of position operator $\mathbf{x}$ , i.e., $\mathbf{x} x\rangle = x x\rangle$ .
<code>spin_coherent(j, theta, phi)</code>	generating spin coherent state as given in Eq. (25).
<code>random(d)</code>	random state with $d$ -dimension following Haar measure.
<code>ghz(n)</code>	generating GHZ state with $n$ qubits, i.e., $\frac{1}{\sqrt{2}}( 00\dots 0\rangle +  11\dots 1\rangle)$ .
<code>w(n)</code>	generating W state with $n$ qubits, i.e., $\frac{1}{\sqrt{n}}( 0\dots 0\rangle +  01\dots 0\rangle + \dots +  0\dots 01\rangle)$ .
<code>dicke(n, k)</code>	generating Dicke state with $n$ qubits, $k$ excited qubits, i.e., $D(n, k) = \binom{n}{k}^{-\frac{1}{2}} \sum_{x \in \{0,1\}^n}  x\rangle$ . For example, $D(3, 2) = \frac{1}{\sqrt{3}}( 011\rangle +  101\rangle +  110\rangle)$ .

## Appendix B: List of quantum operators build-in tqix

Table IV. List of quantum operators build-in tqix

Name	Description
<code>eyex(d)</code>	identify matrix in $d$ -dimension
<code>soper(s, *)</code>	spin- $s$ operators with option <code>*args</code> can be $x, y, z, +, -$ . <code>soper(s)</code> will return an array of spins $x, y, z$
<code>sigmax()</code>	Pauli matrix $\sigma_x$
<code>sigmay()</code>	Pauli matrix $\sigma_y$
<code>sigmaz()</code>	Pauli matrix $\sigma_z$
<code>sigmap()</code>	$\sigma_+$
<code>sigmam()</code>	$\sigma_-$
<code>lowering(d)</code>	lowering (or annihilation) operator in $d$ dimension
<code>raising(d)</code>	raising (or creation) operator in $d$ dimension
<code>displacement(d, alpha)</code>	displacement operator that cut off at $d$ dimension: i.e., $D(\alpha) = e^{\alpha\mathbf{a}^\dagger - \alpha^* \mathbf{a}}$ .
<code>squeezing(d, beta)</code>	squeezing operator that cut off at $d$ dimension: i.e., $S(\beta) = e^{\frac{1}{2}(\beta^* \mathbf{a}^2 - \beta \mathbf{a}^{\dagger 2})}$ .

### III. CODE FOR HUSIMI AND WIGNER VISUALIZATIONS (FIGURE 2)

```
from tqix import *
import numpy as np
```

```
psi = zbasis(10,7)

# 3d visualization
x = [-3, 3]
y = [-3, 3]
husimi_3d(psi, x, y, cmap = cmindex(1), fname
          ='husimi3d.eps')
```

```
wigner_3d(psi, x ,y ,cmap = cmindex(1),fname
='wigner3d.eps')

# Bloch sphere visualization
THETA = [0, np.pi]
PHI = [0, 2* np.pi]
husimi_spin_3d(psi, THETA ,PHI ,cmap =
cmindex(1),fname = 'husimi_sphere.eps')
wigner_spin_3d(psi, THETA ,PHI ,cmap =
cmindex(1),fname = 'wigner_sphere.eps')
```

For cmap, it is ranged from cmindex(1) to cmindex(82) or listed in [74].

#### IV. CODE FOR CALCULATION TIME OF POVM SETS (FIGURE 4)

```
import time
import numpy as np
from tqix import *
import matplotlib.pyplot as plt

N = 100 # number of repeated measurement

# For Pauli and Stoke
dim_p,time_p = [],[]
time_s = [],

for n in range (1,4):
    #n: number of qubits
    dtime_p = 0.0
    dtime_s = 0.0

    for i in range(N):
        state = random(2**n)
        ###
        model = qmeas(state,'Pauli')
        dtime = model.mtime() #measure time
        dtime_p += dtime

        model = qmeas(state,'Stoke')
        dtime = model.mtime()
        dtime_s += dtime

    dtime_p /= float(N)
    dtime_s /= float(N)

    dim_p.append(2**n)
    time_p.append(dtime_p)
    time_s.append(dtime_s)

# For MUB
dim_mub,time_mub = [],[]
for d in (2,3,4,5,7):
    dtime_mub = 0.0
    for i in range(N):
        state = random(d)
        ###
        model = qmeas(state,'MUB')
        dtime = model.mtime()
        dtime_mub += dtime
```

```
dtime_mub /= float(N)

dim_mub.append(d)
time_mub.append(dtime_mub)

# For SIC
dim_sic, time_sic = [],[]
for d in range(2,9):
    dtime_sic = 0.0
    for i in range(N):
        state = random(d)
        ###
        model = qmeas(state,'SIC')
        dtime = model.mtime()
        dtime_sic += dtime

    dtime_sic /= float(N)

    dim_sic.append(d)
    time_sic.append(dtime_sic)

# Plot figure
fig, ax1 = plt.subplots(figsize=(12,6))
ax1.plot(dim_p, time_p, marker = 'o')
ax1.plot(dim_p, time_s, marker = '^')
ax1.plot(dim_mub, time_mub, marker = 's')
ax1.plot(dim_sic, time_sic, marker = 'v')
ax1.legend(('pauli','stoke','mub','sic'))
ax1.set_xlabel('d')
ax1.set_ylabel('time (s)')
plt.savefig('time_povm.eps')
plt.show()
```

#### V. CODE FOR BACK-ENDS (FIGURE 5)

```
from tqix import *
import numpy as np
import matplotlib.pyplot as plt
import time

def func(n):
    fx = []
    x = np.linspace(0,5,n)
    for i in range(n):
        fx.append(np.exp(-x[i]))
    return fx

samp = 1000 #number of sample
ite = 1000 #number iteration

fx = func(samp)
mc_sim = []
cdf_sim = []

for i in fx:
    mc_sim.append(mc(i,ite))

for i in fx:
    temp = []
    for j in range(ite):
        temp.append(randunit()/i)
```

```

cdf_sim.append(cdf(temp))

x = np.linspace(0,5,samp)
fig, ax = plt.subplots(figsize=(12,6))
ax.plot(x,mc_sim,'b+')
ax.plot(x,cdf_sim,'g.')
ax.plot(x, fx, 'r')
ax.legend(("mc", "cdf", "fx"))
ax.set_xlabel('x')
ax.set_ylabel('exponential');
plt.savefig('fig5.eps')
plt.show()

# time check
mc_times = []
cdf_times = []
ites = []
for ite in range(1000,11000,1000):
    mc_start = time.time()
    for i in fx:
        mc_sim.append(mc(i,ite))
    mc_stop = time.time()
    delta = mc_stop - mc_start
    mc_times.append(delta)

    cdf_start = time.time()
    for i in fx:
        temp = []
        for j in range(ite):
            temp.append(randunit()/i)
        cdf_sim.append(cdf(temp))
    cdf_stop = time.time()
    delta = cdf_stop - cdf_start
    cdf_times.append(delta)

    ites.append(ite)

fig, ax1 = plt.subplots(figsize=(12,6))
ax1.plot(ites, mc_times, 'r')
ax1.plot(ites, cdf_times, 'b--')
ax1.legend(("mc", "cdf"))
ax1.set_xlabel('iteration')
ax1.set_ylabel('time (s)')
plt.savefig('inset.eps')
plt.show()

```

## VI. CODE FOR QUANTUM METROLOGY (FIGURE 9)

```

from tqix import *
from numpy import pi
import matplotlib.pyplot as plt

n = 20

```

```

j = n/2

# spin cat state
def cat(j,theta,phi):
    sc = spin_coherent(j,theta,phi)
    scm = spin_coherent(j,pi-theta,phi)
    s = normx(sc + scm)
    return s

# spin observable
# j3[0] = S_x, j3[1] = S_y, j3[2] = S_z
j3 = soper(j)

def u(x):
    return np.exp(-1j*x*j3[2])

t = np.linspace(0, 0.2, 100)
theta = [0.0, 0.15*pi, 0.25*pi, 0.35*pi]
phi = 0.0

# open figures
f1 = plt.figure()
f2 = plt.figure()
ax1 = f1.add_subplot(111,aspect = 0.003)
ax2 = f2.add_subplot(111,aspect = 0.115)
for i in theta:
    r, r2, dt = [], [], []
    for k in t:
        #expectation value j3[1] and j3[1]**2
        model = qmeas(dotx(u(k*pi),cat(j,i,phi)), [j3[1],j3[1]**2])
        ex1 = model.probability()[0]
        ex2 = model.probability()[1]
        r.append(ex1)
        r2.append(ex2)
        dt.append(np.sqrt(np.abs(ex2-ex1**2)))

#differential dr and delta_varphi
dr = ndiff(t,r)
dp = dt/np.abs(dr)

#plot
ax1.plot(t,r,'-')
ax2.plot(t,dp,'--')

#standard quantum limit and Heisenberg limit
sql = 1./np.sqrt(float(n))*np.ones(t.shape)
hl = 1./float(n)*np.ones(t.shape)

ax2.plot(t,sql)
ax2.plot(t,hl)

plt.ylim(0,1)
plt.show()

```

[1] P. Busch, P. Lahti, P. Juha-Pekka, and K. Ylino, *Quantum Measurement* (Springer International Publishing, 2018).

[2] M. A. Nielsen and I. L. Chuang, *Quantum computation and quantum information* (Cambridge University Press, 2010).

- [3] J. A. Wheeler and W. H. Zurek, *Quantum theory and measurement* (Princeton University Press, 2014).
- [4] M. Paris and J. Řeháček (Eds), *Quantum State Estimation*, Lecture Notes in Physics, Vol. 649 (Springer-Verlag, Berlin Heidelberg, 2004).
- [5] V. Giovannetti, S. Lloyd, and L. Maccone, *Nature Photonics* **5**, 222 (2011).
- [6] L. Pezzè, A. Smerzi, M. K. Oberthaler, R. Schmied, and P. Treutlein, *Rev. Mod. Phys.* **90**, 035005 (2018).
- [7] O. S. Magaña-Loaiza and R. W. Boyd, *Reports on Progress in Physics* **82**, 124401 (2019).
- [8] C. L. Degen, F. Reinhard, and P. Cappellaro, *Rev. Mod. Phys.* **89**, 035002 (2017).
- [9] P. Kok, W. J. Munro, K. Nemoto, T. C. Ralph, J. P. Dowling, and G. J. Milburn, *Rev. Mod. Phys.* **79**, 135 (2007).
- [10] A. M. Childs and W. van Dam, *Rev. Mod. Phys.* **82**, 1 (2010).
- [11] S. Pirandola, U. L. Andersen, L. Banchi, M. Berta, D. Bunandar, R. Colbeck, D. Englund, T. Gehring, C. Lupo, C. Ottaviani, J. Pereira, M. Razavi, J. S. Shaari, M. Tomamichel, V. C. Usenko, G. Vallone, P. Villoresi, and P. Wallden, “Advances in quantum cryptography,” (2019), arXiv:1906.01645 [quant-ph].
- [12] D. F. V. James, P. G. Kwiat, W. J. Munro, and A. G. White, *Phys. Rev. A* **64**, 052312 (2001).
- [13] J. Helsen, X. Xue, L. M. K. Vandersypen, and S. Wehner, *npj Quantum Information* **5**, 71 (2019).
- [14] F. Frank, T. Unden, J. Zoller, R. S. Said, T. Calarco, S. Montangero, B. Naydenov, and F. Jelezko, *npj Quantum Information* **3**, 48 (2017).
- [15] A. Gheorghiu, T. Kapourniotis, and E. Kashefi, *Theory of Computing Systems* **63**, 715 (2019).
- [16] A measurement set contains one or several positive-operator-valued measures (POVMs).
- [17] J. Johansson, P. Nation, and F. Nori, *Computer Physics Communications* **183**, 1760 (2012).
- [18] J. Johansson, P. Nation, and F. Nori, *Computer Physics Communications* **184**, 1234 (2013).
- [19] T. Radtke and S. Fritzsche, *Computer Physics Communications* **179**, 647 (2008).
- [20] T. Radtke and S. Fritzsche, *Computer Physics Communications* **181**, 440 (2010).
- [21] S. Fritzsche, *Computer Physics Communications* **185**, 1697 (2014).
- [22] Y. Watanabe, T. Sagawa, and M. Ueda, *Phys. Rev. Lett.* **104**, 020401 (2010).
- [23] R. Harper, S. T. Flammia, and J. J. Wallman, *Nature Physics* (2020), 10.1038/s41567-020-0992-8.
- [24] R. Schmied and P. Treutlein, *New Journal of Physics* **13**, 065019 (2011).
- [25] R. McConnell, H. Zhang, J. Hu, S. Čuk, and V. Vuletić, *Nature* **519**, 439 (2015).
- [26] B. Koczor, R. Zeier, and S. J. Glaser, *Phys. Rev. A* **101**, 022318 (2020).
- [27] S. Ahmed, C. S. Muñoz, F. Nori, and A. F. Kockum, “Classification and reconstruction of optical quantum states with deep neural networks,” (2020), arXiv:2012.02185 [quant-ph].
- [28] H. Moya-Cessa and P. L. Knight, *Phys. Rev. A* **48**, 2479 (1993).
- [29] J. P. Dowling, G. S. Agarwal, and W. P. Schleich, *Phys. Rev. A* **49**, 4101 (1994).
- [30] G. G. Stokes, *Transactions of the Cambridge Philosophical Society* **9**, 399 (1851).
- [31] R. T. Thew, K. Nemoto, A. G. White, and W. J. Munro, *Phys. Rev. A* **66**, 012303 (2002).
- [32] J. Schwinger, *Proceedings of the National Academy of Sciences* **46**, 570 (1959), <https://www.pnas.org/content/46/4/570.full.pdf>.
- [33] I. Bengtsson, *AIP Conference Proceedings* **889**, 40 (2007), <https://aip.scitation.org/doi/pdf/10.1063/1.2713445>.
- [34] Bandyopadhyay, Boykin, Roychowdhury, and Vatan, *Algorithmica* **34**, 512 (2002).
- [35] T. DURT, B.-G. ENGLERT, I. BENGTS-SON, and K. ŻYCZKOWSKI, *International Journal of Quantum Information* **08**, 535 (2010), <https://doi.org/10.1142/S0219749910006502>.
- [36] A. Klappenecker and M. Rötteler, in *Finite Fields and Applications*, edited by G. L. Mullen, A. Poli, and H. Stichtenoth (Springer Berlin Heidelberg, Berlin, Heidelberg, 2004) pp. 137–144.
- [37] J. Lawrence, i. c. v. Brukner, and A. Zeilinger, *Phys. Rev. A* **65**, 032320 (2002).
- [38] J. M. Renes, R. Blume-Kohout, A. J. Scott, and C. M. Caves, *Journal of Mathematical Physics* **45**, 2171 (2004), <https://doi.org/10.1063/1.1737053>.
- [39] H. M. Weyl, *The theory of groups and quantum mechanics: Transl. from the second (rev.) German ed. by H.P. Robertson. With 3 diagrams* (Dover Publ., 1930).
- [40] A. J. Scott and M. Grassl, *Journal of Mathematical Physics* **51**, 042203 (2010), <https://doi.org/10.1063/1.3374022>.
- [41] N. Bent, H. Qassim, A. A. Tahir, D. Sych, G. Leuchs, L. L. Sánchez-Soto, E. Karimi, and R. W. Boyd, *Phys. Rev. X* **5**, 041006 (2015).
- [42] D. M. Appleby, *Journal of Mathematical Physics* **46**, 052107 (2005), <https://doi.org/10.1063/1.1896384>.
- [43] M. Grassl, “On sic-povms and mubs in dimension 6,” (2004), arXiv:quant-ph/0406175 [quant-ph].
- [44] G. Gour and A. Kalev, *Journal of Physics A: Mathematical and Theoretical* **47**, 335302 (2014).
- [45] M. Grassl, *Electronic Notes in Discrete Mathematics* **20**, 151 (2005), proceedings of the Workshop on Discrete Tomography and its Applications.
- [46] G. Zauner, “External links.”
- [47] A. Tavakoli, M. Farkas, D. Rosset, J.-D. Bancal, and M. Kaniewski, “Mutually unbiased bases and symmetric informationally complete measurements in bell experiments: Bell inequalities, device-independent certification and applications,” (2019), arXiv:1912.03225 [quant-ph].
- [48] A. E. Rastegin, *The European Physical Journal D* **67**, 269 (2013).
- [49] I. Bengtsson, *Journal of Physics: Conference Series* **254**, 012007 (2011).
- [50] R. Beneduci, T. J. Bullock, P. Busch, C. Carmeli, T. Heinosaari, and A. Toigo, *Phys. Rev. A* **88**, 032312 (2013).
- [51] W. K. Wootters, *Foundations of Physics* **36**, 112 (2006).
- [52] R. Y. Rubinstein and D. P. Kroese, *Simulation and the Monte Carlo method* (Wiley., 2017).
- [53] K. E. Gentle, *Computational Statistics* (Springer, 2009).
- [54] C. Schwemmer, L. Knips, D. Richart, H. Weinfurter, T. Moroder, M. Kleinmann, and O. Gühne, *Phys. Rev. Lett.* **114**, 080403 (2015).
- [55] P. Faist and R. Renner, *Phys. Rev. Lett.* **117**, 010404 (2016).
- [56] L. Maccone and C. C. Rusconi, *Phys. Rev. A* **89**, 022122 (2014).

- [57] L. B. Ho, *Journal of Physics B: Atomic, Molecular and Optical Physics* **53**, 1106601 (2020)-ph].
- [58] L. B. Ho, *Physics Letters A* **383**, 289 (2019).
- [59] K. Q. Tuan, H. Q. Nguyen, and L. B. Ho, “Direct state measurements under state-preparation-and-measurement errors,” (2020), arXiv:2007.05294 [quant-ph].
- [60] Z. Hradil, *Phys. Rev. A* **55**, R1561 (1997).
- [61] G. Torlai, G. Mazzola, J. Carrasquilla, M. Troyer, R. Melko, and G. Carleo, *Nature Physics* **14**, 447 (2018).
- [62] T. Xin, S. Lu, N. Cao, G. Anikeeva, D. Lu, J. Li, G. Long, and B. Zeng, *npj Quantum Information* **5**, 109 (2019).
- [63] T. Weiss and O. Romero-Isart, *Phys. Rev. Research* **1**, 033157 (2019).
- [64] Y. Liu, D. Wang, S. Xue, A. Huang, X. Fu, X. Qiang, P. Xu, H.-L. Huang, M. Deng, C. Guo, X. Yang, and J. Wu, *Phys. Rev. A* **101**, 052316 (2020).
- [65] Q. Xu and S. Xu, “Neural network state estimation for full quantum state tomography,” (2018), arXiv:1806.06661 [quant-ph].
- [66] Y. Quek, S. Fort, and H. K. Ng, “Adaptive quantum state tomography with neural networks,” (2018), arXiv:1812.06693 [quant-ph].
- [67] S. L. Braunstein and C. M. Caves, *Phys. Rev. Lett.* **72**, 3439 (1994).
- [68] S. L. Braunstein, *Journal of Physics A: Mathematical and General* **28**, 761 (1995).
- [69] J. Huang, X. Qin, H. Zhong, Y. Ke, and C. Lee, *Scientific Reports* **5**, 17894 (2015).
- [70] J. Huang, M. Zhuang, B. Lu, Y. Ke, and C. Lee, *Phys. Rev. A* **98**, 012129 (2018).
- [71] L. B. Ho and Y. Kondo, *Physics Letters A* **383**, 153 (2019).
- [72] Y. Lee Loh and M. Kim, *American Journal of Physics* **83**, 30 (2015), <https://doi.org/10.1119/1.4898595>.
- [73] J. Huang, M. Zhuang, and C. Lee, *Phys. Rev. A* **97**, 032116 (2018).
- [74] “<https://matplotlib.org/tutorials/colors/colormaps.html>,” .